BIOCHEMISTRY
including biophysical chemistry & molecular biology
Article

Biochemistry **2009,** *48,* 4789–4797 4789
DOI: 10.1021/bi900299f

Observation of "Ionic Lock" Formation in Molecular Dynamics Simulations of Wild-Type β_1 and β_2 Adrenergic Receptors[†]

Stefano Vanni, Marilisa Neri, Ivano Tavernelli, and Ursula Rothlisberger*

Laboratory of Computational Chemistry and Biochemistry, Federal Institute of Technology, EPFL, CH-1015 Lausanne, Switzerland

Received February 20, 2009; Revised Manuscript Received April 6, 2009

ABSTRACT: G protein coupled receptors (GPCRs) are a large family of integral membrane proteins involved in signal transduction pathways, making them appealing drug targets for a wide spectrum of diseases. The recently crystallized structures of two engineered adrenergic receptors have opened new avenues for the understanding of the molecular mechanisms of action of GPCRs. Taking the two crystal structures as a starting point, we carried out submicrosecond molecular dynamics simulations of wild-type β_1 and β_2 adrenergic receptors in a lipid bilayer under physiological conditions. These simulations give access to structural and dynamic properties of the receptors in pseudo in vivo conditions. For both systems the overall fold properties of the transmembrane region as well as the binding pocket remain close to the crystal structure of the engineered systems, thus suggesting that the ligand binding mode is not affected by the introduced modifications. Both simulations indicate the presence of one or two internal water molecules absent in both crystal structures and essential for the stabilization of the binding pocket at the interface between transmembrane helices III, IV, and V. The different interactions arising from the substitution of Tyr308 in β_2AR into Phe325 in β_1AR induce different conformations of the homologous Asn(6.55) inside the binding pockets of the two receptors, suggesting a possible origin of receptor specificity in agonist binding. The equilibrated structures of both receptors recover all of the previously suggested features of inactive GPCRs including formation of a salt bridge between the cytoplasmatic moieties of helices III and VI ("ionic lock") that is absent in the crystal structures.

G protein coupled receptors are the largest family of integral membrane receptors responsible for signal transduction into the cell, and they play a crucial role in many essential and diverse physiological processes, ranging from neurotransmission to cell growth. As a consequence, they are drug targets for a wide spectrum of diseases (*1*). Among them, β adrenergic receptors are crucial for cardiovascular and pulmonary function regulation through the binding of catecholamines, such as the endogenous hormone adrenaline or the neurotransmitter noradrenaline.

In particular, distinction between β_1 and β_2 adrenergic receptors is based upon their relative affinities for these two catecholamine agonists as well as on their relative distribution in cell tissue. Differences in β_1AR and β_2AR are responsible for their different role upon agonist activation (mainly heart muscle contraction for β_1AR and smooth muscle relaxation for β_2AR), and the development of β-blockers able to bind selectively among the two receptors is a major focus in drug development (*2*).

Three-dimensional structures of GPCRs[1] have been very difficult to obtain despite many efforts, and until recently rhodopsin was the only GPCR for which crystallographic data were available (*3*). As a consequence, analysis of the dynamical properties at the atomistic scale of such proteins was only possible via computational techniques based on homology modeling with rhodopsin as a template (*4*, *5*).

Recently, Stevens et al. (*6*) and Schertler et al. (*7*) were able to resolve the crystal structures of β_2 and β_1 adrenergic receptors, thus opening a large field of potential studies and applications regarding structure and function of GPCRs able to bind diffusible ligands. The procedures followed to achieve crystallization of the two highly homologous receptors (*8*, *9*) imply different experimental modifications of the native system (i.e., engineering with a lysozyme or an antibody (*10*) in the third intracellular loop for β_2AR and several single point mutations for β_1AR). In both cases, partial or total deletion of the third intracellular loop, which is known to interact with G proteins, was crucial to achieve crystallization. Since these modifications perturb the activity of the receptors with respect to the in vivo environment, stand alone analysis of the crystallographic data seems insufficient to draw definitive conclusions on the relationship between structure and function (*6*, *7*, *11*, *12*). In particular,

[†]Support from the Swiss National Science Foundation (Grant 200020-116294) is gratefully acknowledged.

*To whom correspondence should be addressed. E-mail: ursula.roethlisberger@epfl.ch. Phone: (41) 21 69 30 321. Fax: (41) 21 69 30 320.

[1]Abbreviations: GPCR, G protein coupled receptor; β_2AR, β_2 adrenergic receptor; β_1AR, β_1 adrenergic receptor; AR, adrenergic receptor; BRET, bioluminescence resonance energy transfer; FRET, fluorescence resonance energy transfer; MD, molecular dynamics; TM, transmembrane; FTIR, Fourier-transform infrared spectroscopy; rmsd, root-mean-square deviation; RMSF, root-mean-square fluctuation; ICL, intracellular loop; ECL, extracellular loop; WT, wild type; T4L, T4 lysozyme chimera; SOPE, 1-stearoyl-2-oleoyl-*sn*-glycero-3-phosphoethanolamine.

Published on Web 04/20/2009

T4L-β_2AR lysozyme chimera exhibits WT affinity for antagonists and inverse agonists but 2-to-3-fold higher affinity for both agonists and partial agonists (*8*). The mutant β_1AR-m23, on the other hand, binds antagonists with similar affinities to that of the WT receptor while the agonists noradrenaline and isoprenaline bind more weakly by a factor of 2470 and 650 (*9*), respectively.

Even though the specificity of catecholamine-binding ARs is well studied (*13*) and several experiments (*14*−*18*) have shown which residues are crucial in agonist and antagonist binding, to date no atomistic explanation of the observed specificity is available. Moreover, although the binding mode of the partial inverse agonist carazolol and of the high-affinity antagonist cyanopindolol can be inferred from the crystal structures (*6*, *7*), some questions arise from this static picture of the binding pocket. In particular, the side chain rotamer conformation of Ser203 in β_2AR is unexpectedly different from the conformation adopted in the β_1AR crystal structure by the homologous residue Ser211 (*7*). At the same time, the dynamic properties of the binding pocket as well as the role of water remain largely unknown (*19*, *20*). Interestingly, in spite of the distinct specificities of β_1AR and β_2AR, a comparison between the binding pockets of the two receptors shows that only one residue in the immediate surrounding of the ligand[1] is different (Phe325 in β_1AR equivalent to Tyr308 in β_2AR), but it does not directly interact with the bound ligand.

The multistep process leading to GPCR activation is still unclear, and the common framework to describe receptor activation is the so-called extended ternary complex model (*21*), which proposes an equilibrium between inactive and active states. Several experiments (*22*−*33*) identified a number of conserved regions in GPCRs, disruption of which could lead to a shift in the active/inactive equilibrium of the receptor. Among them, the conformational transition of Trp(6.48) of the CWxP motif in TM6 (the "rotamer toggle switch"), the interaction pattern of Asn (7.49) and Tyr(7.53) of the NPxxY motif in TM7, and the salt bridge ("ionic lock") between Arg(3.50) of the (D/E)RY motif of TM3 and the partially conserved Glu(6.30) in the cytoplasmatic end of TM6. Quite surprisingly, the crystal structures of the two adrenergic receptors (ARs), that are bound to an inverse agonist and to an antagonist and are thus likely to be representative of the inactive conformation of the receptor, are lacking the salt bridge between the cytoplasmatic ends of TM3 and TM6, a feature that was suggested by previous experiments as a key representative of the inactive state of such receptors (*22*, *24*, *32*, *34*−*40*).

Molecular dynamics simulations of transmembrane proteins embedded in a lipid bilayer with explicit solvent and counterions provide a realistic representation of the protein in its native environment (*41*), and previous MD studies (*42*−*44*) have supplied insights into the function and the activation mechanisms of GPCR-like systems. To investigate the global structural stability of the binding pocket and the atomistic binding modes of different ligands as well as the dynamical properties of the receptors, we carried out 0.5 μs molecular dynamics simulations of monomeric (*45*) wild-type β_2AR and β_1AR in a lipid bilayer. For the latter system, we also performed simulations of the β_1AR mutant that was used to achieve crystallization. Although the limited time scales of MD simulations (hundreds of nanoseconds) are not able to capture the overall process of activation of ARs (that includes time scales of the order of milliseconds), they can give insights about the behavior of wild-type receptors and help in detecting possible structural and dynamic differences between the two highly homologous receptors.

[1]Defined as within 5 Å from the ligand in the crystal structure.

METHODS

All simulations are based on the crystal structure of human β_2 adrenergic receptor (Protein Data Bank code 2RH1) obtained at 2.4 Å resolution after replacement of the third intracellular loop with a T4-lysozyme chimera (T4L-β_2AR) (*6*) and on chain B of the crystal structure of partially mutated (R68S, M90V, Y227A, A282L, F327A, F338M) turkey β_1 adrenergic receptor (Protein Data Bank code 2VT4) solved at 2.7 Å resolution (β_1AR-m23). MODELLER9v3 (*46*−*48*) was used to add missing amino acid residues 16−29 in the N-terminal and residues 342−353 in the C-terminal tail of β_2AR; amino acid residues 1−15 and 354−365 that are also missing in the X-ray structure were not included. The same software package has been used to model the third intracellular loop (234−259), choosing the loop with the lowest DOPE score (*49*) among the ones not overlapping with the explicit membrane. The same procedure was used for the β_1AR, where residues 31−38 in the N-terminus and residues 360−367 in the C-terminus were added, while residues 1−30, absent in the crystal structure, were not included. The third intracellular loop (residues 239−243 and 272−283) was modeled, maintaining the same deletion (residues 244−271) that was used to achieve crystallization. For wild-type β_1AR, residues Ser68, Val90, Ala227, Leu282, Ala327, and Met338 were mutated back to Arg68, Met90, Tyr227, Ala282, Phe327, and Phe338.

In both receptors, all ionizable side chains and the C- and N-termini are in their default ionization states, except for Asp (2.50) and Glu(3.41). Asp(2.50) is assumed to be protonated on the basis of FTIR experiments carried out on the homologous receptor rhodopsin that suggest that Asp(2.50) is protonated in both dark and MetaII rhodopsin(*50*). The protonation state of Glu(3.41), that is located in TM3 and is particularly close to TM4 and to the membrane environment, has been studied by carrying out MD simulations of both possible protomers in the case of β_2AR; in fact, while Poisson−Boltzmann analysis suggests that the residue is carrying a net negative charge (*6*), FTIR experiments on the homologous Glu122 of rhodopsin suggest that this residue is protonated in both rhodopsin and metarhodopsin (*50*). Analysis of the overall rmsd of TM4 (that interacts directly with the side chain of Glu122 in the simulation where the residue is charged) and of rmsd of residues within 5 Å of the side chain of Glu(3.41) in the crystal structure suggests that Glu(3.41) is protonated in the native form of the receptor. All histidine residues present in the proteins are assumed to be protonated either in the N_δ position (His22, His269, His296 for β_2AR; His180 for β_1AR) or in the N_ε position (His18, His93, His172, His178, His241, His256 for β_2AR; His286 in β_1AR). The net charge of carazolol (Figure 1a) and cyanopindolol (Figure 1b) has been set to +1 e.

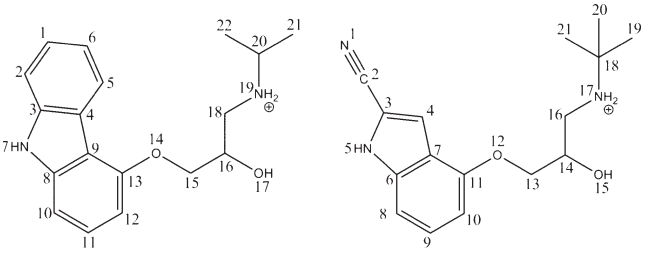

FIGURE 1: Carazolol (left) and cyanopindolol (right) structures and corresponding numbering schemes.

An overall neutral system at physiological ion concentration (100 mmol/L) was obtained adding 20 sodium and 30 chloride ions to the aqueous phase for the β_2AR simulation, while 14 sodium and 30 chloride ions were added in the β_1AR system. Heteroatoms (as defined in the PDB format) present in the crystal structures are not included in the model, except for internal water molecules, the ligands, and a palmitic acid residue bound to Cys341 for β_2AR. The program Dowser (*51*) was used to locate internal cavities in the protein and to assess their hydrophilicity by means of calculating the interaction energy of a water molecule with the surrounding atoms. A water molecule was placed in a cavity if the interaction energy was stronger than −10 kcal/mol. By this criterion, which has been found to be able to distinguish well hydrated from empty cavities (*42*, *51*), five water molecules in addition to the ones resolved in the crystal structure were added for β_2AR, while in the case of β_1AR, 13 water molecules in addition to the seven crystallographic ones were added (Figure 2).

The lipids used for the membrane simulation are 1-stearoyl-2-oleoyl-*sn*-glycero-3-phosphoethanolamine (SOPE). The length of the aliphatic tail was chosen in such a way as to optimize the hydrophobic matching between the protein and the lipid bilayer. The system was immersed in a box of water of approximately 90 × 90 × 105 Å^3 containing 16000 molecules. The box dimensions are chosen in such a way that the minimum distance between periodic images of the protein is always larger than 30 Å during the simulation. The protein was inserted into the membrane such that helix VIII lies at the hydrophobic/hydrophilic interface, with the hydrophilic residues pointing toward the aqueous phase. The total number of atoms in our models is about 90000.

The all-atom AMBER/parm99SB (*52*) force field was used for the proteins, carazolol and cyanopindolol, whereas the AMBER/parm96 was used for the lipid bilayer in combination with the SPC (*53*) model for water. The force field for the palmitic acid was taken from previous studies (*42*). The atomic charges for carazolol and cyanopindolol were derived by RESP (*52*, *54*, *55*) fitting using HF/6-31G* optimized structures and electrostatic potentials obtained using the Gaussian03 package (*56*).

All data collections and equilibration runs were done using GROMACS 4 (*57*). Electrostatic interactions were calculated with the Ewald particle mesh method (*58*), with a real space cutoff of 12 Å. Bonds involving hydrogen atoms were constrained using the LINCS (*59*) algorithm, and the time integration step was set to 2 fs. The system was coupled to a Nosé−Hoover thermostat (*60*, *61*) and to an isotropic Parrinello−Rahman barostat (*62*) at a temperature of 310 K and a pressure of 1 atm.

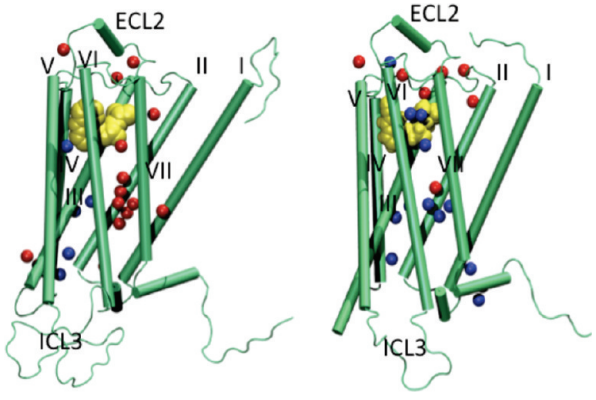

FIGURE 2: β_2AR (left) and β_1AR (right) tertiary structures with the ligands carazolol and cyanopindolol (yellow), crystal water molecules (red), and internal water molecules placed by Dowser (*51*) (blue).

After insertion of the protein in a preequilibrated lipid bilayer, the system was minimized using steepest descent algorithm and then heated to 310 K in 1040 ps while keeping positional restraints on crystallographic C_α and ligand heavy atoms. The constraints were removed slowly during three sets of 3 ns runs. Finally, the equilibration run was completed with a 6 ns run with positional restraints applied to the ligand heavy atoms.

All data analyses were done using GROMACS (*57*) utilities, and all molecular images were made with Visual Molecular Dynamics (VMD) (*63*).

RESULTS

Native Structure. To understand the dynamic properties of the native structures of the receptors, we have carried out MD simulations of β_1AR-m23 and of wild-type β_1AR and β_2AR. Simulations on the hundreds of nanoseconds time scale in pseudo in vivo environment indicate that the global fold properties of the receptors suggested by the two crystal structures are retained along the simulations despite the engineering techniques used for crystallization. Equilibration of the system could be obtained with only small deviations from the X-ray structures even though significant equilibration times (50−100 ns) are required. Specifically, the backbone rmsd of the seven transmembrane helices of the equilibrated geometry is less than 1.2 Å for wild-type β_2AR, around 1 Å for wild-type β_1AR, and 1.5 Å for β_1AR-m23 (see Supporting Information).

In addition, rmsd analysis of the different TM helices suggests that TM6 and TM7 are mainly responsible for deviations from the crystal structure as they display the greatest mobility among all TMs. This is consistent with the high β-factor of the intracellular moiety of TM7 and TM6 and can be a consequence of the artifacts introduced by the modeling of the third intracellular loop (ICL3) that is missing in the crystal structure. This is particularly true in the simulation of β_2AR where the ICL3 fragment is 26 residues long. Equilibration of such a long intracellular loop requires extensive simulation times, and even if the rmsd of ICL3 reaches a plateau in our simulations, this may not correspond to the equilibrium conformation of the loop in the native receptor. Nevertheless, the low value for the global backbone rmsd of TM5 and TM6 (lower than 1.5 Å in all cases) suggests that the conformation of this loop does not affect the fold properties of the transmembrane region in a significant way in the time scales we have investigated here.

A number of specific characteristic features suggested by the two crystal structures are retained throughout the simulations, among them, the direct hydrophobic interactions between the ligands and ECL2 that lock this loop into a fairly rigid conformation (in both receptors) and the presence of a sodium ion within ECL2 coordinated by the backbone carbonyl groups of residues Cys192, Asp195, and Cys198 and two water molecules (in β_1AR). In particular, it is remarkable that the overall rmsd of the two active sites (defined by including residues within 5 Å from the ligands in the crystal structure) is extremely low, oscillating around 1 Å in all of the simulations (data in Supporting Information). Moreover, both hydrophobic interactions as well as the hydrogen bond network between the ligand and the receptors remain nearly unchanged during 500 ns of simulation time for the three systems.

These considerations strongly suggest that both engineering techniques used to achieve crystallization do not induce significant modifications in the structure of the receptors with respect to

the wild types and that the conformation of the binding site and the description of the binding modes constitute a reliable starting point for further investigations.

Binding Mode. The precise binding mode of diffusible ligands in class A GPCRs is not yet completely known. The crystal structures of the two ARs have confirmed that Asp(3.32) and Asn(7.39) form a complementary H-bond (defined by a N−O distance cutoff of 3 Å and an angle cutoff of 20°) network with the ethanolamine group of the ligands (Figure 3 shows the interaction pattern for carazolol in the β_2AR binding pocket), where Asn(7.39) acts both as a H-bond acceptor and donor to the amine nitrogen and hydroxyl oxygen of the ligands and Asp(3.32) is a H-bond acceptor for the protonated amine nitrogen and the hydroxyl group of the ligands. The carbazole heterocycle of carazolol and the indole derivative moiety of cyanopindolol interact with Phe(6.52) via an edge-to-face π stacking (Figure 4) while the carbazole and the indole nitrogen atoms of the ligands act as a H-bond donor for the carboxyl oxygen of the Ser(5.42) side chain (Figure 3).

Unrestrained MD simulations of carazolol-bound β_2AR and of cyanopindolol-bound β_1AR, carried out for 500 ns, show that the hydrogen bond network between the ethanolamine group of the ligands and residues Asp(3.32) and Asn(7.39) is conserved during the simulation time, thus showing a high stability even under realistic conditions. In particular, the MD simulations highlight the role of Tyr(7.43), a residue highly conserved among class A GPCRs(*64*), that does not interact directly with the ligands but stabilizes Asp(3.32) acting as H-donor to form an hydrogen bond with one of the two carboxyl oxygens of Asp (3.32) as already suggested from inspection of the crystal structures (Figure 3).

While the N−C−C−OH motif is shared by many adrenergic receptor agonists and antagonists, the carbazole and the indole moieties of the ligands and their binding mode with the other amino acids in the binding pocket might contribute for the specificity of the inverse activity of carazolol and the antagonist activity of cyanopindolol, respectively. These peculiar interactions are achieved by both tight interactions between the carbazole and the indole rings and hydrophobic residues as well as by an important hydrogen bond between the nitrogen atom of the carbazole and indole moieties and the side chain oxygen of Ser (5.42) (Figure 3). The side chain conformation of Ser(5.42), and in particular the dihedral angle formed between the side chain O_γ atom and the C_β, C_α, and C, is different in the crystals of the two ARs. This hydrogen bond is conserved along the whole trajectory in all of the simulations, and the most stable conformation is the one found in the crystal structure of β_1AR-m23. This peculiar interaction pattern is stabilized by a network of hydrogen bonds between the side chains of Ser(5.42), Ser(5.46), and Tyr(5.38), the backbone oxygen of Tyr(5.38), and one or two water molecules present in the cavity between TM3, TM4, and TM5 (Figure 5) that enter the binding site during the simulations. The role of these water molecules is crucial to stabilize the inverse agonist/antagonist interaction network at the interface between TM3, TM4, and TM5 (Figure 5), especially the backbone−backbone interaction between Ser(5.42) and Ser(5.46). It is worth mentioning that one of these internal water molecules is present in chains A and D of the crystal structure of β_1AR, while it is absent both in chain B and in chain C of β_1AR and in the crystal structure of β_2AR. This feature may be specific for inverse agonist/antagonist binding while in the case of agonists a different binding mode has been suggested (*10*).

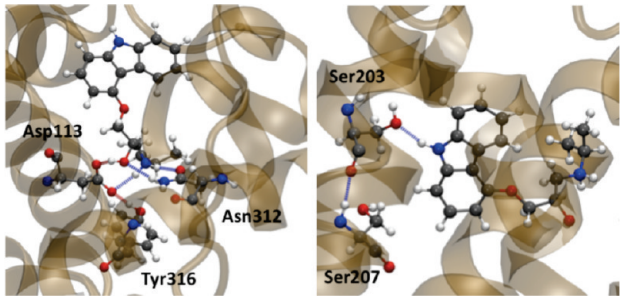

FIGURE 3: Hydrogen bond interactions between carazolol, Asp113 (3.32), Asn312(7.39), and Tyr316(7.43) (on the left) and with Ser203 (5.42) and Ser207(5.46) (on the right).

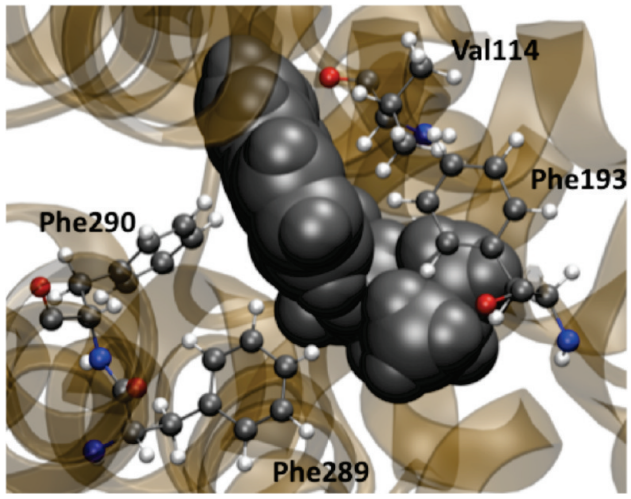

FIGURE 4: View from the extracellular side of hydrophobic interactions between carazolol (in space-filling representation) and residues Val114(3.33), Phe193(5.32), Phe289(6.51), and Phe290(6.52).

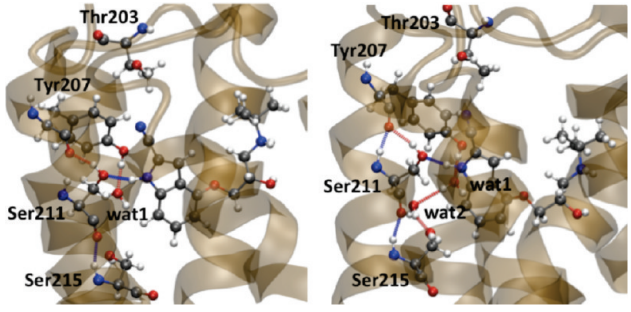

FIGURE 5: Hydrogen bonds between cyanopindolol and residues Thr203(5.34), Tyr207(5.38), Ser211(5.42), and Ser215(5.46) with one water molecule present in the cavity (left) or two water molecules present in the cavity (right).

At the same time, the X-ray structures show tight hydrophobic packing between the ligands and a series of surrounding residues (Trp(3.28), Val(3.33), Val(3.36), Phe(5.32), Thr(5.34), Tyr(5.38), Phe(5.47) Trp(6.48), Phe(6.51), Phe(6.52), and Ile(7.36)). Among these, the role of Val(3.33) (Figure 4) is crucial, since it has been shown that mutation of this residue into Ala decreases β_2AR affinity toward the antagonist alprenolol by 1 order of magnitude and lowers affinity for the agonist adrenaline 300-fold (*18*).

MD simulations show that this tight hydrophobic packing (Figure 4) leads to a well-preserved orientation of the ligands in the binding pocket, where the only, limited, mobility is the thermally allowed rotary movement of the isopropyl tail of carazolol and the *tert*-butyl tail of cyanopindolol.

Interestingly, one of the residues located between the ligand and the extracellular aqueous environment is Phe(5.32) (Figure 4), which maintains hydrophobic interactions with the ligand. This residue could be involved in the regulation of ligand entry in the binding pocket. It belongs to the short α-helix present in the second extracellular loop (Figure 4), a secondary structure element that is peculiar to β adrenergic receptors and that is absent in all rhodopsin crystal structures.

Receptor Specificity. The binding mode suggested by the crystal structures is consistent with earlier site-directed mutagenesis studies that highlighted the role of Asp(3.32), Asn(7.39), and Ser(5.42) in both agonist and antagonist binding (*15*−*17*) (Figure 3). Moreover, Ser(5.43), Ser(5.46), and Asn(6.55) that are supposedly (*14*, *65*, *66*) not involved in antagonist binding (while being crucial for agonist binding) are indeed located in the binding pocket but do not interact directly with the ligand.

Interestingly, the immediate surroundings of the binding pocket (defined as all amino acids within 5 Å from the ligand) are fully conserved with the sole exception of Tyr308(7.35) in β_2AR that is mutated into Phe325(7.35) in β_1AR. Mutagenesis studies (*66*, *67*) suggest that Tyr308 in β_2AR plays a role in agonist selectivity. This residue is located in the proximity of the charged nitrogen of the ligand at the interface between the active site and the solvent (Figure 6) within hydrogen bond distance from Asn(6.55), another residue known to be crucial in agonist binding (*65*).

Due to the different physical interactions with Tyr308, respectively Phe325, the conformation of Asn(6.55) is different in the two simulations. In β_2AR a stable hydrogen bond between the hydroxyl group of Tyr308 and the side chain oxygen of Asn(6.55) assists in keeping the binding site in a closely packed conformation around the ligand (Figure 6). As a result of this interaction, the amine group of Asn(6.55) can assume different possible conformations; the absence of a fixed conformation for Asn (6.55) might rationalize the marginal role of this residue in antagonist/inverse agonist interactions (*65*). Residue Phe325 in β_1AR, on the other hand, cannot form hydrogen bonds with Asn (6.55), a residue that is stabilized by a hydrogen bond (either as hydrogen donor or hydrogen acceptor) with the side chain of Ser (5.43), another residue that is known to be involved in agonist binding as indicated by mutagenesis studies (*14*).

These results indicate that the effects that the replacement of Tyr308 by Phe325 has on Asn(6.55) could induce in turn a different interaction between this residue and the hydroxyl groups of the catechol moiety of the agonists adrenaline and noradrenaline, thus suggesting a possible origin of the specificity of β_1AR versus β_2AR in agonist binding.

Further differences between β_1AR and β_2AR can be found in the extracellular side that controls ligand access to the binding pocket. This region is also remarkably different in the two AR crystal structures when compared to rhodopsin. In particular, the two packed β-sheets that are shielding the active site of rhodopsin from water to prevent hydrolysis of the covalently bound protonated Schiff base of *cis*-retinal are replaced, in adrenergic receptors, by a long loop forming a helix that lies on top of the active site and directly contributes to the tight hydrophobic packing around the ligand via Phe(5.32).

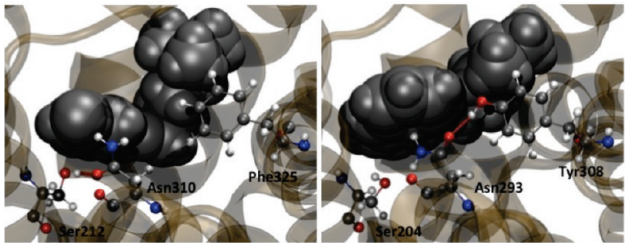

FIGURE 6: Preferred conformations of Asn310(6.55) and Phe325 (7.35) in β_1AR (left) and conformation of Asn293(6.55) and Tyr308 (7.35) in β_2AR (right).

The stabilization of this channel is achieved in different ways in the two adrenergic receptors. Key differences are the salt bridge formed in β_2AR between Asp192(5.31) and Lys305(7.32) that is present in β_2AR but not in β_1AR, as well as the peculiar interaction achieved in β_1AR arising from coordination of a sodium ion by the backbone carbonyl groups of residues located in ICL2 (Cys192, Asp195, Cys198) and two water molecules. Simulations show that these interactions are strictly preserved along the dynamics.

Activation/Inhibition Model. It is generally accepted that rhodopsin, the most studied G protein coupled receptor, undergoes a bimodal activation mechanism, where the active (R*) state is reached starting from the inactive (R) state after photoinduced isomerization of the retinal in the binding pocket via a series of collective movements that involve the transmembrane helices and the intracellular loops (*21*). Rhodopsin can be activated by a single photon, but in the absence of light it has no detectable basal activity. On the other hand, adrenergic receptors, like many GPCRs, show a considerable amount of basal, agonist-independent activity. In addition, a large class of substances are able to alter the ability of adrenergic receptors to activate a given signaling pathway; in particular, agonists are able to fully activate the receptor, partial agonists induce submaximal activation of the G protein even at saturation concentrations, inverse agonists inhibit basal activity, while antagonists have no effect on basal activity but competitively block the access of other ligands.

Many GPCR activation mechanisms have been proposed in the literature (*5*, *22*−*24*, *27*, *32*, *33*, *36*−*38*, *68*), but there is no consensus about their generality, the time scale in which they occur, and whether they are all essential to activate a given signaling pathway. The most studied and generally acknowledged activation mechanisms for adrenergic receptors are the conformational transition of Trp(6.48) in the CWxP motif in TM6 (the "rotamer toggle switch"), the modulation of the pattern of interactions of the NPxxY motif of TM7 and the internal water molecules linking Trp(6.48), Asp(2.50), and the NPxxY motif, and the breaking of the salt bridge ("ionic lock") between Arg(3.50) in the (D/E)RY motif of TM3 and the conserved Glu(6.30) in the cytoplasmatic end of TM6.

Moreover, the recently solved crystal structure of ligand-free opsin in its G-protein interacting conformation(*69*) has confirmed that outward movement of the intracellular part of TM6 (that tilts outward by 6−7 Å with respect to the structure of dark rhodopsin) is required for activation. This movement enables Arg (3.50) to adopt an extended conformation pointing toward the protein core and to interact directly with the G-protein. This conformation is further stabilized by a conformational change of Tyr(5.58) and Tyr(7.53) that move toward the protein core getting closer to Arg(3.50) and, in the case of Tyr(5.58), forming a new hydrogen bond with the positively charged residue.

The systems studied in this work should represent adrenergic receptors in slightly different functional states. Wild-type β_2AR with the bound inverse agonist carazolol and β_1AR-m23 with the bound antagonist cyanopindolol should mimic the inactive state

of the receptors while wild-type β_1AR with the bound antagonist cyanopindolol should represent a less inactive conformation.

Quite surprisingly, the crystal structures of the two adrenergic receptors do not completely reproduce all of the characteristics that were thought to be representative of the inactive form of GPCRs. In particular, while Trp(6.48) and the pattern of interaction of the NPxxY motif are very similar to the inactive form of rhodopsin and consistent with previous studies on different GPCRs (*19*, *27*, *35*, *70*), the interhelical cytoplasmic distance between TM3 and TM6 in the two adrenergic receptors is larger than in inactive rhodopsin (Table 1), thus preventing formation of the salt bridge between Arg(3.50) of the (D/E)RY motif of TM3 and Glu(6.30).

In all of our simulations, the conformation of Trp(6.48) does not change, thus retaining the inactive-like state that was found in both crystal structures. A pair of conserved (*19*) internal water molecules create a stable hydrogen bond network connecting Trp (6.48) with the highly conserved Asp(2.50) (Figure 7). The interaction between Asp(2.50) and Asn(7.49) of the NPxxY motif has been suggested as a crucial step in the activation process of thyrotropin receptor (*27*), with Asn(7.49) undergoing a gauche−trans isomerization that allows for direct interaction with Asp (2.50) in the active conformation of the receptor. In agreement with these observations, we do not see any such direct interaction in our simulations, thus confirming that the systems under investigation are likely to represent inactive states of the receptors.

At the same time, it has been proposed that Tyr(7.53) of the NPxxY motif, situated at the cytoplasmatic end of TM7, must directly interact with TM2 in the inactive state of β_2AR, based on analogy with the crystal structure of rhodopsin and MD simulations (*70*). This interaction is not present in either of the crystal structures of β_2AR and β_1AR. In our simulations, we observe that Tyr(7.53) is indeed changing conformation with respect to the crystal structures (Figure 7) pointing toward TM2 and, in the case of wild-type β_2AR, is directly interacting with Asn(2.40).

On the other hand, the crystal structure of active opsin (*69*) suggests that Tyr(5.58), that is located in the intracellular moiety of TM5, can play a role in the activation mechanism. In particular, this residue points toward the lipid-exposed side of TM6 in dark rhodopsin, while it is directly pointing toward the protein core in the opsin crystal structure, directly hydrogen bonding Arg(3.50). Interestingly, in the crystal structure of β_2AR-T4L this residue lies between TM3 and TM6 in an opsin-like conformation, while it has been mutated to an alanine in the crystal structure of β_1AR-m23. In both simulations of reconstructed wild-type receptors, Tyr(5.58) adopts a stable conformation that is similar to the one found in the crystal structure of inactive rhodopsin, pointing toward the TM5−TM6 interface. In this conformation, the hydroxyl moiety of Tyr(5.58) forms a stable hydrogen bond with the backbone oxygen of Leu (6.34) that stabilizes the TM5−TM6 interface. It must be noted that simulations of β_1AR-m23, where Tyr(5.58) is mutated into an alanine, suggest that this TM5−TM6 stabilization can be replaced by formation of an hydrogen bond between the hydroxyl of Tyr(5.62) and the backbone oxygen of Lys(6.35).

However, the most studied and widely accepted activation mechanism is the disruption of the network of interactions ("ionic lock") located at the cytoplasmic interface between TM3 and TM6 in the highly conserved (D/E)RY amino acid sequence. Evidence for such a mechanism, both in rhodopsin and in adrenergic receptors, has been collected by a variety of studies including site-directed mutagenesis (*22*, *34*, *39*), fluorescence spectroscopy (*35*, *40*, *71*), site-directed spin labeling (*38*), and double electron−electron resonance (*36*), as well as analysis of available crystal structures of rhodopsin and its apoform opsin (Table 1).

Table 1: $C_\alpha-C_\alpha$ Distance between Arg(3.50) and Glu(6.30) in Available Crystal Structures of GPCRs in the Protein Data Bank and from MD Simulations[a]

GPCR	data origin	PDB ID	functional state	$C_\alpha-C_\alpha$ "ionic-lock" distance (Å)
rhodopsin	X-ray	1F88(3)	inactive	8.7
rhodopsin	X-ray	1U19(72)	inactive	9.1
rhodopsin	X-ray	2G87(73)	batho	9.0
rhodopsin	X-ray	2HPY(74)	lumi	9.1
rhodopsin	X-ray	2I37(75)	photoactivated deprotonated intermediate	10.6
opsin	X-ray	3CAP(69)	active	15.0
β_2AR-4TL	X-ray	2RH1(6)	hybrid	11.2
β_1AR-m23	X-ray	2VT4(7)	inactive	11.0
β_1AR-m23	MD		inactive	7.7
β_2AR-wt	MD		inactive	7.3
β_1AR-wt	MD		inactive/partially active	9.8

[a] Corresponding to the average value over the final 100 ns.

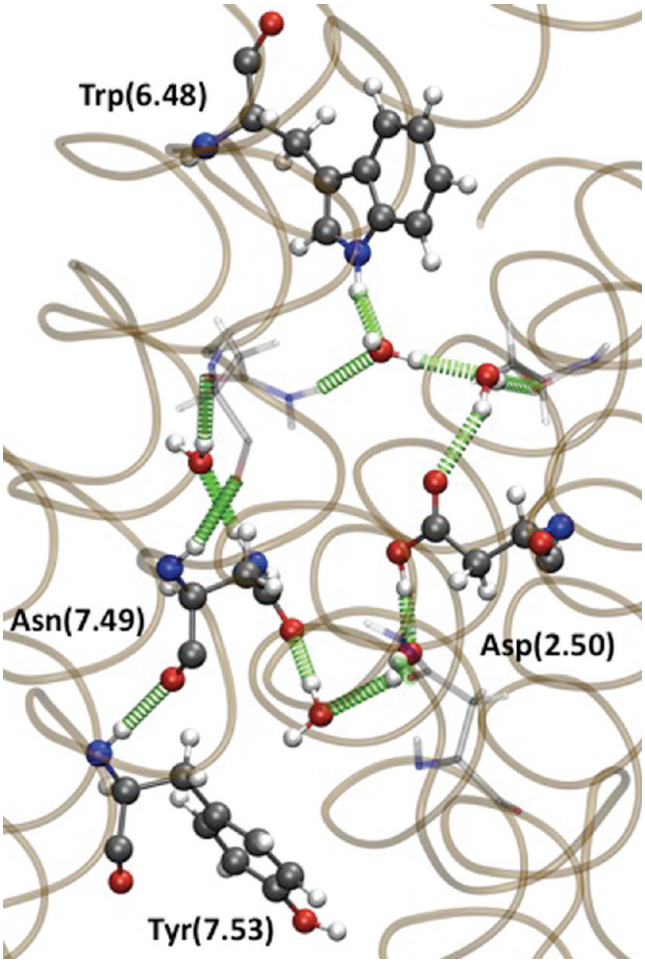

FIGURE 7: Water-mediated hydrogen bond network between Trp (6.48), Asp(2.50), Asn(7.49), and Tyr(7.53).

Surprisingly, the crystal structures of the two adrenergic receptors are lacking such a "lock", and the $C_\alpha-C_\alpha$ distance between Arg(3.50) and Glu(6.30) that has been suggested as a better marker than the mere salt bridge formation (*7*) (due to the

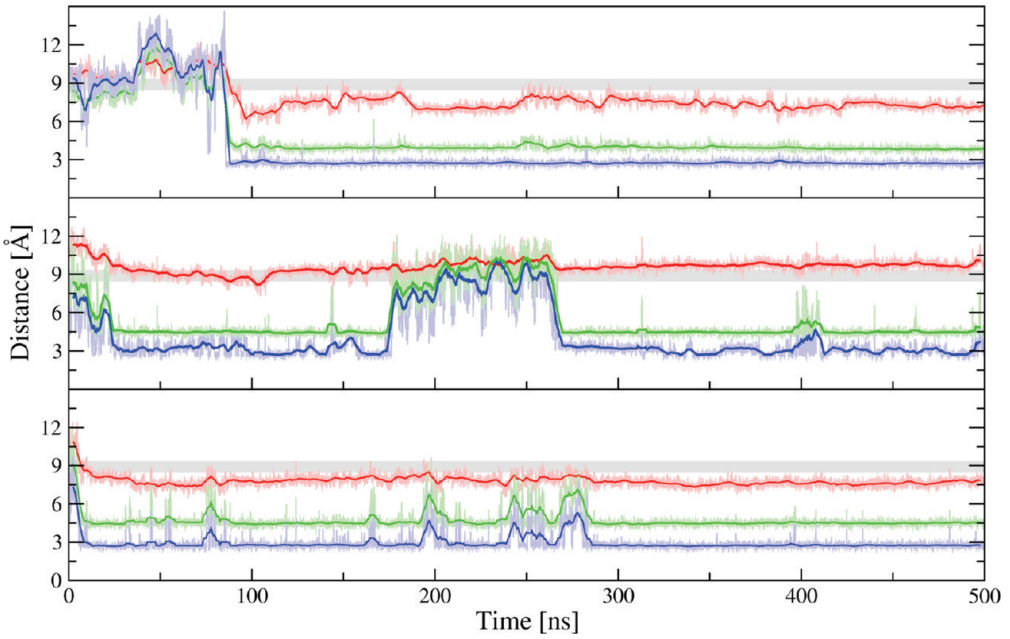

FIGURE 8: Time evolution of $C_\alpha-C_\alpha$ (red), $C_\zeta-C_\delta$ (green), and $N_\eta-O_\delta$ (blue) distances between Arg(3.50) and Glu(6.30) for carazolol-bound β_2AR-wt (upper panel), cyanopindolol-bound β_1AR-wt (medium panel), and β_1AR-m23 (lower panel). Averages are shown in corresponding solid lines. The shadowed gray bar represents the $C_\alpha-C_\alpha$ distance of crystal strucutures of inactive rhodopsin (see Table 1).

high β factor of the two residues) is larger than in the inactive forms of rhodopsin (Table 1). As a consequence, formation of the Arg(3.50)−Glu(6.30) salt bridge cannot be achieved by mere side chain rotation, but it must be driven by collective movements of the transmembrane helices.

Our simulations show indeed formation of the ionic lock, with the cytoplasmatic end of TM6 approaching TM3 resulting in an equilibrium geometry that is stabilized by direct interaction of Arg(3.50) and Glu(6.30).[3] Moreover, the stable conformations of β_2AR and β_1AR-m23, that should mimic the inactive configuration of the receptor, show a $C_\alpha-C_\alpha$ distance between Arg(3.50) and Glu(6.30) (Figure 8) that is comparable with the X-ray structures of inactive rhodopsin (Figure 8). In wild-type β_1AR, instead, TM3 and TM6 are closer than in the crystal structure, and although the "ionic lock" between the two side chains is formed, the $C_\alpha-C_\alpha$ distance is larger than in inactive rhodopsin, in agreement with the consideration that wild-type β_1AR bound to cyanopindolol does not keep the receptor in a completely inactive conformation.

Combined mutational and FTIR experiments on rhodopsin (*28*) suggested that disruption of the intrahelical salt bridge between Arg(3.50) and Glu(3.49) is considerably more critical for shifting the equilibrium to the active conformation than disruption of the "ionic lock" between TM3 and TM6. Our simulations support these considerations, and the salt bridge between Arg(3.50) and Glu(3.49) is well conserved along the trajectories.

[3]It has also been suggested (*7*, *28*) that crystal packing effects could be responsible for the misfolding of ICL2 in the crystal structure of β_2AR and that this could lead to a non-native position of a conserved tyrosine (Tyr149 in β_1AR, Tyr141 in β_2AR). The side chain of this tyrosine forms a hydrogen bond with Asp(3.49) in β_1AR (where the ICL2 shows a well-structured α-helical conformation) while it is located between Glu(6.30) and Arg(3.50) in the crystal structure of β_2AR. Our simulations show that while in β_1AR the interaction between this tyrosine and Asp(3.49) is extremely stable, in β_2AR the tyrosine moves away, thus allowing formation of the salt bridge between Glu(6.30) and Arg(3.50); at the same time the side chain of Ser143 in ICL2 forms direct hydrogen bonds to Asp(3.49), thus replacing the role of Tyr149 in β_1AR.

CONCLUSIONS

With the recent crystal structures of β adrenergic receptors (*6*, *7*) as a starting point, our simulations provide for the first time an atomistic picture of the dynamics of the unengineered form of G protein coupled receptors able to bind diffusible ligands.

Despite the sequence differences between the engineered forms that have been crystallized and the reconstructed wild-type receptors, the wild-type receptors remain extremely close to the X-ray structure, and only small deviations can be noticed over hundreds of nanoseconds of simulation time. In particular, MD simulations show that the ligand binding mode suggested by the crystal structures of both engineered receptors remains basically unchanged throughout the simulation time.

The average rmsd of the binding pockets with respect to the crystal structures is smaller than 1.2 Å for both receptors. This relative rigidity of the active site is achieved via a stable network of hydrogen bond interactions (residues Asp(3.32), Asn(7.39), and Ser(5.42)) as well as through a number of hydrophobic contacts.

The distinctly different orientation of Asn(6.55) in the two receptors, induced by the interaction arising from the substitution of a tyrosine into a phenylalanine, is extremely conserved along the dynamics and might play a decisive role for β adrenergic receptor specificity.

All of the previously proposed characteristics of the inactive form of such receptors are observed in the simulations. In particular, the MD simulations reconfirm that the most stable conformation of inactive adrenergic receptors under pseudo in vivo conditions involves formation of a salt bridge between the cytoplasmatic moieties of TM3 and TM6.

Our results suggest that both crystal structures are a viable starting point for further computational studies such as in silico docking or MD investigations of the mechanisms of agonist binding or receptor activation. However, it must be pointed out that getting an atomistic comprehension of the function of such receptors via MD simulations is all but straightforward, due to the long simulation time required and the need for a careful and extensive equilibration.

ACKNOWLEDGMENT

We thank Pablo Campomanes for reading the manuscript and Matteo Guglielmi for testing the topology of the membrane used in this study.

SUPPORTING INFORMATION AVAILABLE

rmsd time series of TM helix backbone and of binding pocket for β_2AR-wt, β_1AR-wt, and β_1AR-m23. This material is available free of charge via the Internet at http://pubs.acs.org.

REFERENCES

1. Pierce, K. L., Premont, R. T., and Lefkowitz, R. J. (2002) Seven-transmembrane receptors. *Nat. Rev. Mol. Cell Biol. 3*, 639–650.
2. Taylor, M. R. G. (2007) Pharmacogenetics of the human beta-adrenergic receptors. *Pharmacogenomics J. 7*, 29–37.
3. Palczewski, K., Kumasaka, T., Hori, T., Behnke, C. A., Motoshima, H., Fox, B. A., Le Trong, I., Teller, D. C., Okada, T., Stenkamp, R. E., Yamamoto, M., and Miyano, M. (2000) Crystal structure of rhodopsin: A G protein-coupled receptor. *Science 289*, 739–745.
4. Spijker, P., Vaidehi, N., Freddolino, P. L., Hilbers, P. A. J., and Goddard, W. A. (2006) Dynamic behavior of fully solvated beta-2-adrenergic receptor, embedded in the membrane with bound agonist or antagonist. *Proc. Natl. Acad. Sci. U.S.A. 103*, 4882–4887.
5. Bhattacharya, S., Hall, S. E., Li, H., and Vaidehi, N. (2008) Ligand-stabilized conformational states of human beta(2) adrenergic receptor: Insight into G-protein-coupled receptor activation. *Biophys. J. 94*, 2027–2042.
6. Cherezov, V., Rosenbaum, D. M., Hanson, M. A., Rasmussen, S. G., Thian, F. S., Choi, H. J., Kuhn, P., Weis, W. I., Kobilka, B. K., and Stevens, R. C. (2007) High-resolution crystal structure of an engineered human beta2-adrenergic G protein-coupled receptor. *Science 318*, 1258–1265.
7. Warne, T., Serrano-Vega, M. J., Baker, J. G., Moukhametzianov, R., Edwards, P. C., Henderson, R., Leslie, A. G. W., Tate, C. G., and Schertler, G. F. X. (2008) Structure of a beta1-adrenergic G-protein-coupled receptor. *Nature 454*, 486–491.
8. Rosenbaum, D. M., Cherezov, V., Hanson, M. A., Rasmussen, S. G. F., Thian, F. S., Kobilka, T. S., Choi, H. J., Yao, X. J., Weis, W. I., Stevens, R. C., and Kobilka, B. K. (2007) GPCR engineering yields high-resolution structural insights into beta(2)-adrenergic receptor function. *Science 318*, 1266–1273.
9. Serrano-Vega, M. J., Magnani, F., Shibata, Y., and Tate, C. G. (2008) Conformational thermostabilization of the beta 1-adrenergic receptor in a detergent-resistant form. *Proc. Natl. Acad. Sci. U.S.A. 105*, 877–882.
10. Rasmussen, S. G. F., Choi, H. J., Rosenbaum, D. M., Kobilka, T. S., Thian, F. S., Edwards, P. C., Burghammer, M., Ratnala, V. R. P., Sanishvili, R., Fischetti, R. F., Schertler, G. F. X., Weis, W. I., and Kobilka, B. K. (2007) Crystal structure of the human beta(2) adrenergic G-protein-coupled receptor. *Nature 450*, 383–U384.
11. Weis, W. I., and Kobilka, B. K. (2008) Structural insights into G-protein-coupled receptor activation. *Curr. Opin. Struct. Biol. 18*, 734–740.
12. Xiang, Y., and Kobilka, B. (2005) The beta-adrenergic receptors: Lessons from knockouts. *Adrenergic receptors in the 21st century,* 267–291.
13. Kobilka, B. K., and Deupi, X. (2007) Conformational complexity of G-protein-coupled receptors. *Trends Pharmacol. Sci. 28*, 397–406.
14. Strader, C. D., Candelore, M. R., Hill, W. S., Sigal, I. S., and Dixon, R. A. F. (1989) Identification of 2 serine residues involved in agonist activation of the beta-adrenergic-receptor. *J. Biol. Chem. 264* 13572–13578.
15. Strader, C. D., Sigal, I. S., Candelore, M. R., Rands, E., Hill, W. S., and Dixon, A. F. (1988) Conserved aspartic acid residues 79 and 113 of the beta-adrenergic receptor have different roles in receptor function. *J. Biol. Chem. 263*, 10267–10271.
16. Suryanarayana, S., and Kobilka, B. K. (1993) Amino-acid substitutions at position 312 in the 7th hydrophobic segment of the beta(2)-adrenergic receptor modify ligand-binding specificity *Mol. Pharmacol. 44*, 111–114.
17. Liapakis, G., Ballesteros, J. A., Papachristou, S., Chan, W. C., Chen, X., and Javitch, J. A. (2000) The forgotten serine - A critical role for Ser-203(5.42) in ligand binding to and activation of the beta(2)-adrenergic receptor. *J. Biol. Chem. 275*, 37779–37788.
18. Chelikani, P., Hornak, V., Eilers, M., Reeves, P. J., Smith, S. O., RajBhandary, U. L., and Khorana, H. G. (2007) Role of group-conserved residues in the helical core of beta(2)-adrenergic receptor. *Proc. Natl. Acad. Sci. U.S.A. 104*, 7027–7032.
19. Pardo, L., Deupi, X., Doelker, N., Lopez-Rodriguez, M. L., and Campillo, M. (2007) The role of internal water molecules in the structure and function of the rhodopsin family of G protein-coupled receptors. *ChemBioChem 8*, 19–24.
20. Huber, T., Menon, S., and Sakmar, T. P. (2008) Structural basis for ligand binding and specificity in adrenergic receptors: Implications for GPCR-targeted drug discovery. *Biochemistry 47*, 11013–11023.
21. Samama, P., Cotecchia, S., Costa, T., and Lefkowitz, R. J. (1993) A mutation induced activated state of the beta(2)-adrenergic receptor—Extending the ternary complex model. *J. Biol. Chem. 268*, 4625–4636.
22. Ballesteros, J. A., Jensen, A. D., Liapakis, G., Rasmussen, S. G. F., Shi, L., Gether, U., and Javitch, J. A. (2001) Activation of the beta(2)-adrenergic receptor involves disruption of an ionic lock between the cytoplasmic ends of transmembrane segments 3 and 6. *J. Biol. Chem. 276*, 29171–29177.
23. Lei, S., Liapakis, G., Xu, R., Guarnieri, F., Ballesteros, J. A., and Javitch, J. A. (2002) beta(2) adrenergic receptor activation - Modulation of the proline kink in transmembrane 6 by a rotamer toggle switch. *J. Biol. Chem. 277*, 40989–40996.
24. Shapiro, D. A., Kristiansen, K., Weiner, D. M., Kroeze, W. K., and Roth, B. L. (2002) Evidence for a model of agonist-induced activation of 5-hydroxytryptamine 2A serotonin receptors that involves the disruption of a strong ionic interaction between helices 3 and 6 *J. Biol. Chem. 277*, 11441–11449.
25. Scheer, A., Costa, T., Fanelli, F., De Benedetti, P. G., Mhaouty-Kodja, S., Abuin, L., Nenniger-Tosato, M., and Cotecchia, S. (2000) Mutational analysis of the highly conserved arginine within the Glu/Asp-Arg-Tyr motif of the alfa1b-adrenergic receptor: Effects on receptor isomerization and activation. *Mol. Pharmacol. 57*, 219–231.
26. Barak, L. S., Menard, L., Ferguson, S. S. G., Colapietro, A. M., and Caron, M. G. (1995) The conserved seven-transmembrane sequence NP(X)2,3Y of the G-protein-coupled receptor superfamily regulates multiple properties of the beta(2)-adrenergic receptor. *Biochemistry 34*, 15407–15414.
27. Urizar, E., Claeysen, S., Deupi, X., Govaerts, C., Costagliola, S., Vassart, G., and Pardo, L. (2005) An activation switch in the rhodopsin family of G protein-coupled receptors. *J. Biol. Chem. 280*, 17135–17141.
28. Vogel, R., Mahalingam, M., Ludeke, S., Huber, T., Siebert, F., and Sakmar, T. P. (2008) Functional role of the "ionic lock" - An interhelical hydrogen-bond network in family A heptahelical receptors. *J. Mol. Biol. 380*, 648–655.
29. Proulx, C. D., Holleran, B. J., Boucard, A. A., Escher, E., Guillemette, G., and Leduc, R. (2008) Mutational analysis of the conserved Asp2.50 and ERY motif reveals signaling bias of the urotensin II receptor. *Mol. Pharmacol. 74*, 552–561.
30. Bihoreau, C., Monnot, C., Davies, E., Teutsch, B., Bernstein, K. E., Corvol, P., and Clauser, E. (1993) Mutation of Asp74 of the rat angiontensin II receptor confers changes in antagonist affinities and abolishes G-protein coupling. *Proc. Natl. Acad. Sci. U.S.A. 90* 5133–5137.
31. Baker, J. G., Proudman, R. G. W., Hawley, N. C., Fischer, P. M., and Hill, S. J. (2008) Role of key transmembrane residues in agonist and antagonist actions at the two conformations of the human beta(1)-adrenoceptor. *Mol. Pharmacol. 74*, 1246–1260.
32. Greasley, P. J., Fanelli, F., Rossier, O., Abuin, L., and Cotecchia, S. (2002) Mutagenesis and modelling of the alpha(1b)-adrenergic receptor highlight the role of the helix 3/helix 6 interface in receptor activation. *Mol. Pharmacol. 61*, 1025–1032.
33. Fritze, O., Filipek, S., Kuksa, V., Palczewski, K., Hofmann, K. P., and Ernst, O. P. (2003) Role of the conserved NPXXY(x)(5,6)F motif in the rhodopsin ground state and during activation. *Proc. Natl. Acad. Sci. U.S.A. 100*, 2290–2295.
34. Rasmussen, S. G. F., Jensen, A. D., Liapakis, G., Ghanouni, P., Javitch, J. A., and Gether, U. (1999) Mutation of a highly conserved aspartic acid in the beta(2) adrenergic receptor: Constitutive activation, structural instability, and conformational rearrangement of transmembrane segment 6. *Mol. Pharmacol. 56*, 175–184.
35. Yao, X. J., Parnot, C., Deupi, X., Ratnala, V. R. P., Swaminath, G., Farrens, D., and Kobilka, B. (2006) Coupling ligand structure to specific conformational switches in the beta(2)-adrenoreceptor. *Nat. Chem. Biol. 2*, 417–422.
36. Altenbach, C., Kusnetzow, A. K., Ernst, O. P., Hofmann, K. P., and Hubbell, W. L. (2008) High-resolution distance mapping in rhodopsin reveals the pattern of helix movement due to activation. *Proc. Natl. Acad. Sci. U.S.A. 105*, 7439–7444.

37. Swaminath, G., Deupi, X., Lee, T. W., Zhu, W., Thian, F. S., Kobilka, T. S., and Kobilka, B. (2005) Probing the beta(2) adrenoreceptor binding site with catechol reveals differences in binding and activation by agonists and partial agonists. *J. Biol. Chem. 280*, 22165–22171.
38. Farrens, D. L., Altenbach, C., Yang, K., Hubbell, W. L., and Khorana, H. G. (1996) Requirement of rigid-body motion of transmembrane helices for light activation of rhodopsin. *Science 274* 768–770.
39. Kim, J. M., Altenbach, C., Thurmond, R. L., Khorana, H. G., and Hubbell, W. L. (1997) Structure and function in rhodopsin: Rhodopsin mutants with a neutral amino acid at E134 have a partially activated conformation in the dark state. *Proc. Natl. Acad. Sci. U. S.A. 94*, 14273–14278.
40. Ghanouni, P., Steenhuis, J. J., Farrens, D. L., and Kobilka, B. K. (2001) Agonist-induced conformational changes in the G-protein-coupling domain of the beta(2) adrenergic receptor. *Proc. Natl. Acad. Sci. U.S.A. 98*, 5997–6002.
41. Gumbart, J., Wang, Y., Aksimentiev, A., Tajkhorsid, E., and Schulten, K. (2005) Molecular dynamics simulations of proteins in lipid bilayers. *Curr. Opin. Struct. Biol. 15*, 423–431.
42. Rohrig, U., Guidoni, L., and Rothlisberger, U. (2002) Early steps of the intramolecular signal transduction in rhodopsin explored by molecular dynamics simulations. *Biochemistry 41*, 10799–10809.
43. Lin, Y. C., Cao, Z. X., and Mo, Y. R. (2006) Molecular dynamics simulations on the *Escherichia coli* ammonia channel protein AmtB: Mechanism of ammonia/ammonium tranport. *J. Am. Chem. Soc. 128*, 10876–10884.
44. Noskov, S. Y., Berneche, S., and Roux, B. (2004) Control of ion selectivity in potassium channels by electrostatic and dynamic properties of carbonyl ligands. *Nature 431*, 830–834.
45. Whorton, M. R., Bokoch, M. P., Rasmussen, S. G. F., Huang, B., Zare, R. N., Kobilka, B., and Sunahara, R. K. (2007) A monomeric G protein-coupled receptor isolated in a high-density lipoprotein particle efficiently activates its G protein. *Proc. Natl. Acad. Sci. U.S.A. 104*, 7682–7687.
46. Fiser, A., Do, R. K., and Sali, A. (2000) Modeling of loops in protein structures. *Protein Sci. 9*, 1753–1773.
47. Marti-Renom, M. A., A., S., Fiser, A., Sanchez, R., Melo, F., and Sali, A. (2000) Comparative protein strucure modeling of genes and genomes. *Annu. Rev. Biophys. Biomol. Struct. 29*, 291–325.
48. Sali, A., and Blundell, T. L. (1993) Comparative protein modelling by satisfaction of spatial restraints. *J. Mol. Biol. 234*, 779–815.
49. Shen, M. Y., and Sali, A. (2006) Statistical potential for assessment and prediction of protein structures. *Protein Sci. 15*, 2507–2524.
50. Fahmy, K., Jager, F., Beck, M., Zvyaga, T. A., Sakmar, T. P., and Siebert, F. (1993) Protonation states of membrane-embedded carboxylic-acid groups in rhodopsin nad metarhodopsin-II—A Fourier-transform infrared spectroscopy study of site-directed mutants. *Proc. Natl. Acad. Sci. U.S.A. 90*, 10206–10210.
51. Zhang, L., and Hermans, J. (1996) Hydrophilicity of cavities in proteins. *Proteins: Struct., Funct., Genet. 24*, 433–438.
52. Cornell, W. D., Cieplak, P., Bayly, C. I., Gould, I. R., Merz, K. M., Ferguson, D. M., Spellmeyer, D. C., Fox, T., Caldwell, J. W., and Kollman, P. A. (1995) A 2nd generation force-field for the simulation of proteins, nucleic-acids, and organic-molecules. *J. Am. Chem. Soc. 117*, 5179–5197.
53. Berendsen, H. J. C., Postma, J. P. M., Vangunsteren, W. F., and Hermans, J. (1981) Interaction models for water in relation to protein hydration. *Intermolecular Forces,* 331–342.
54. Bayly, C. I., Cieplak, P., Cornell, W. D., and Kollman, P. A. (1993) A well-behaved electrostatic potential based method using charge restraints for deriving atomic charges - The RESP model. *J. Phys. Chem. 97*, 10269–10280.
55. Wang, J. M., Cieplak, P., and Kollman, P. A. (2000) How well does a restrained electrostatic potential (RESP) model perform in calculating conformational energies of organic and biological moelcules?. *J. Comput. Chem. 21*, 1049–1074.
56. Frisch, M. J. T., G. W., Schlegel, H. B., Scuseria, G. E., Robb, M. A., Cheeseman, J. R., Montgomery, Jr., J. A., Vreven, T., Kudin, K. N., Burant, J. C., Millam, J. M., Iyengar, S. S., Tomasi, J., Barone, V., Mennucci, B., Cossi, M., Scalmani, G., Rega, N., Petersson, G. A., Nakatsuji, H., Hada, M., Ehara, M., Toyota, K., Fukuda, R., Hasegawa, J., Ishida, M., Nakajima, T., Honda, Y., Kitao, O., Nakai, H., Klene, M., Li, X., Knox, J. E., Hratchian, H. P., Cross, J. B., Bakken, V., Adamo, C., Jaramillo, J., Gomperts, R., Stratmann, R. E., Yazyev, O., Austin, A. J., Cammi, R., Pomelli, C., Ochterski, J. W., Ayala, P. Y., Morokuma, K., Voth, G. A., Salvador, P., Dannenberg, J. J., Zakrzewski, V. G., Dapprich, S., Daniels, A. D., Strain, M. C., Farkas, O., Malick, D. K., Rabuck, A. D., Raghavachari, K., Foresman, J. B., Ortiz, J. V., Cui, Q., Baboul, A. G., Clifford, S., Cioslowski, J., Stefanov, B. B., Liu, G., Liashenko, A., Piskorz, P., Komaromi, I., Martin, R. L., Fox, D. J., Keith, T., Al-Laham, M. A., Peng, C. Y., Nanayakkara, A., Challacombe, M., Gill, P. M. W., Johnson, B., Chen, W., Wong, M. W., Gonzalez, C., and Pople, J. A. (2004) Gaussian 03 Gaussian, Inc., Wallingford, CT.
57. Van der Spoel, D., Lindahl, E., Hess, B., Groenhof, G., Mark, A. E., and Berendsen, H. J. C. (2005) GROMACS: Fast, flexible and free *J. Comput. Chem. 26*, 1701–1718.
58. Essmann, U., Perera, L., Berkowitz, M. L., Darden, T., Lee, H., and Pedersen, L. G. (1995) A smooth particle mesh ewald method *J. Chem. Phys. 103*, 8577–8593.
59. Hess, B., Bekker, H., Berendsen, H. J. C., and Fraaije, J. G. E. M. (1997) LINCS: A linear constraint solver for molecular simulations. *J. Comput. Chem. 18*, 1463–1472.
60. Nose, S. (1986) An extension of the canonical ensemble molecular-dynamics method. *Mol. Phys. 57*, 187–191.
61. Hoover, W. G. (1985) Canonical dynamics - Equilibrium phase-space distributions. *Phys. Rev. A 31*, 1695–1697.
62. Parrinello, M., and Rahman, A. (1981) Polymorphic transitions in single-crystals - A new molecular-dynamics method. *J. Appl. Phys. 52*, 7182–7190.
63. Humphrey, W., Dalke, A., and Schulten, K. (1996) VMD - Visual molecular dynamics. *J. Mol. Graphics 14*, 33–38.
64. Horn, F., Van der Wenden, E. M., Oliveira, L., IJzerman, A. P., and Vriend, G. (2000) Receptors coupling to G proteins: Is there a signal behind the sequence?. *Proteins: Struct., Funct., Genet. 41*, 448–459.
65. Wieland, K., Zuurmond, H. M., Krasel, C., Ijzerman, A. P., and Lohse, M. J. (1996) Involvement of Asn-293 in stereospecific agonist recognition and in activation of the beta2-adrenergic receptor. *Proc. Natl. Acad. Sci. U.S.A. 93*, 9276–9281.
66. Isogaya, M., Yamagiwa, Y. M., Fujita, S., Sugimoto, Y., Nagao, T., and Kurose, H. (1998) Identification of a key amino acid of the beta (2)-adrenergic receptor for high affinity binding of salmeterol *Mol. Pharmacol. 54*, 616–622.
67. Kikkawa, H., Isogaya, M., Nagao, T., and Kurose, H. (1998) The role of the seventh transmembrane region in high affintiy binding of a beta (2)-selective agonist TA-2005. *Mol. Pharmacol. 53*, 128–134.
68. Azzi, M., Charest, P. G., Angers, S., Rousseau, G., Kohout, T., Bouvier, M., and Pineyro, G. (2003) Beta-arrestin-mediated activation of MAPK by inverse agonists reveals distinct active conformations for G protein-coupled receptors. *Proc. Natl. Acad. Sci. U.S.A. 100*, 11406–11411.
69. Park, J. H., Scheerer, P., Hofmann, K. P., Choe, H. W., and Ernst, O. P. (2008) Crystal structure of the ligand-free G-protein-coupled receptor opsin. *Nature 454*, 183–U133.
70. Han, D. S., Wang, S. X., and Weinstein, H. (2008) Active state-like conformational elements in the beta(2)-AR and a photoactivated intermediate of rhodopsin identified by dynamic properties of GPCRs. *Biochemistry 47*, 7317–7321.
71. Ghanouni, P., Gryczynski, Z., Steenhuis, J. J., Lee, T. W., Farrens, D. L., Lakowicz, J. R., and Kobilka, B. K. (2001) Functionally different agonists induce distinct conformations in the G protein coupling domain of the beta(2) adrenergic receptor. *J. Biol. Chem. 276*, 24433–24436.
72. Okada, T., Sugihara, M., Bondar, A. N., Elstner, M., Entel, P., and Buss, V. (2004) The retinal conformation and its environment in rhodopsin in light of a new 2.2 Å crystal structure. *J. Mol. Biol. 342*, 571–583.
73. Nakamichi, H., and Okada, T. (2006) Crystallographic model of bathorhodopsin. *Angew. Chem., Int. Ed. Engl. 45*, 4270–4273.
74. Nakamichi, H., and Okada, T. (2006) Local peptide movement in the photoreaction intermediate of rhodopsin. *Proc. Natl. Acad. Sci. U.S. A. 103*, 12728–12734.
75. Salom, D., Lodowski, D. T., Stenkamp, R. E., Le Trong, I. Golczak, M., Jastrzebska, B., Harris, T., Ballesteros, J. A., and Palczewski, K. (2006) Crystal strcuture of a photoactivated deprotonated intermediate of rhodopsin. *Proc. Natl. Acad. Sci. U.S.A. 103*, 16123–16128.